Defective Nb_2C MXene Anchored Cu Sites Enhancing Photocatalytic CO_2 Reduction to Ethanol

Jiajun Du,[a] Jun Deng,[a] Sharafat Ali, [a] Chang-An Zhou,[a] Hairong Yue,[a] Patrik Schmuki,[b,a] Xuemei Zhou[a]*

[a]School of Chemical Engineering, Sichuan University, No. 24 South Section 1, Yihuan Road, Chengdu, 610065 (P.R.C.). *Email: xuemeizhou@scu.edu.cn.

[b]Friedrich-Alexander-University of Erlangen-Nuremberg, Department of Materials Science and Engineering, Martensstraße 7, 91058 Erlangen, Germany.

1 Experimental section:

1.1 Chemicals and materials

Anhydrous Copper(II) Chloride ($CuCl_2$, 98%), ethanol (C_2H_5OH, 99.7%), P25, Nb_2AlC (99.8%) and Tetrabutylammonium Hydroxide (TBAOH, 10%) were purchased from Adamas. HF (49.9%), NaOH (96%), $NaHCO_3$ (99%) and concentrated hydrochloric acid (HCl, 37 wt.%) were purchased from Chron in Chengdu. And ultrapure water (Resistivity: 17.38 MΩ cm) was utilized in the synthetic process. All reagents were used as received without further purification.

1.2 Synthesis of catalysts

Synthesis of $NbC_{0.67}$ MXene (M). The synthesis of M involved two sequential steps: etching and delamination. Etching: When the HF solution was heated to 55°C, 1 g of Nb_2AlC powder was slowly and carefully added to a PTFE conical flask to react with the HF solution. The addition process lasted 5-10 min to prevent excessive reaction heat. After completion, the flask opening was covered with plastic film pierced with 2-3 small holes. The reaction mixture was continuously stirred for 48 h in a water bath maintained at 55° C. Following acidic etching, the resulting solid was repeatedly washed with ultrapure deionized water and ethanol, followed by centrifugation at 5000 rpm until the supernatant pH approached neutrality to remove excess HF. Delamination: To obtain delaminated M, the synthesized multi-layered niobium carbide powder was dispersed in 10 mL of a 25% tetrabutylammonium hydroxide (TBAOH) solution and vigorously stirred at room temperature for 72 h. Subsequently, the dispersion was centrifuged at 13,000 rpm and washed with ethanol and distilled water to remove TBAOH, retaining the solid. The obtained solid was then dispersed in ultrapure deionized water and ultrasonicated for 1 h under an ice-water bath and N_2 atmosphere. Finally, the ultrasonicated dispersion was centrifuged at 3200 rpm for 20 min to collect the few-layer M aqueous dispersion. M powder was obtained via freeze-drying under vacuum.

Synthesis of Cu-$NbC_{0.67}$ MXene (CuM). Vacuum-freeze-dried M powder was dispersed

in anhydrous ethanol to form a colloidal suspension (1 mg/mL). A calculated amount of 0.5 mg/mL $CuCl_2$ ethanol solution was then added dropwise to the M colloidal solution under continuous stirring. After purging with N_2 for 10 min, the mixture was stirred overnight in a sealed glass vial. The product was centrifuged at 13,000 rpm and washed to remove unreacted $CuCl_2$. The collected powder was redispersed in a minimal volume of water and freeze-dried under vacuum to yield the final CuM.

Sample nomenclature based on Cu loading: M with varying Cu loadings were denoted according to the atomic ratio of Cu to Nb in the precursor: 1% CuM (Cu:Nb = 1:100); 2% CuM (Cu:Nb = 1:50); 10% CuM (Cu:Nb = 1:10).

Synthesis of Cu-$NbC_{0.67}$/P25 (CuMP25). The CuMP25 composite was prepared by a wet deposition method as follows: 100 mg of P25 powder was added to 30 mL of anhydrous ethanol and ultrasonicated for 10 min to form a uniformly dispersed P25 suspension. The pH of the suspension was adjusted to ~5.5 using dilute hydrochloric acid. Under continuous stirring and N_2 purging, 5 mL of a 1 mg/mL CuM ethanolic dispersion was added slowly to the P25 suspension, to give a nominal loading of 5% of CuM on P25. Distinct flocculation of P25 was observed, accompanied by a gradual color change of the powder from white to grayish-blue. After continuous stirring for 2 h, the solid was collected by centrifugation and washed three times with ultrapure deionized water. The product was then dried overnight in a vacuum oven at 80° C to obtain the final CuMP25 composite. The nominal CuM loading (1%, 2%, 10%, 20%) refers to the atomic ratio of Cu to Nb in the precursor solution used for surface redox deposition.

1.3 Material characterizations

Morphology of all samples were observed on a field emission scanning electron microscope (FESEM) (JEOL, JSM-7500, Japan). Transmission electron microscope (TEM) images were acquired with a Japan JEOL-F200 at an acceleration voltage of 200 KV. Samples were dispersed in ethanol, and 10 μL suspension was dropped on an ultra-thin carbon film supported by 300 mesh copper TEM grid and dried for 1 h under

an IR light. Powder X-ray diffraction (XRD) patterns were recorded on a Rigaku MiniFlex600 instrument equipped with a Cu Kα radiation (λ = 0.154178 nm) in the 2θ range of 10° -80° with a step size of 0.01°. The lattice spacing d was calculated by Bragg's law: 2dsinθ=nλ. X-ray photoelectron spectroscopy (XPS) was performed on a Thermo Scientific K-Alpha instrument with a monochromatic Al Kα X-ray source (12 KV, 6 mA). The vacuum of the analysis room is 5.0 × 10^{-7} mbar. The binding energy of all spectra was calibrated to the binding energy of C 1*s* at 284.8 eV.

1.4 Photocatalytic reduction of CO_2

The CO_2 reduction experiments were conducted in a gas-liquid-solid reaction mode using a top-irradiated 250 mL Pyrex batch reactor (Labsolar 6A, Beijing PerfectLight Technology Co., Ltd.). The reaction temperature was maintained at 5°C using circulating cooling water. A 300 W Xe lamp equipped with an AM 1.5 filter provided irradiation with a light power density of 100 mW·cm^{-2}. 20 mg of catalyst powder was dispersed in 3 mL of deionized water (or 0.1 M $NaHCO_3$ solution) and transferred to a glass dish (diameter: 3 cm, depth: 1.5 cm) placed at the reactor bottom. After sealing, the reactor was evacuated for 10 min and purged three times with high-purity CO_2 (99.999%) to eliminate air. Following re-evacuation, CO_2 was continuously introduced until the internal pressure reached ~50 kPa. During illumination, 1 mL of gas was sampled hourly and quantitatively analyzed using an online gas chromatograph (GC2030, Shimadzu, Japan) equipped with a Carboxen® 1010 PLOT capillary column (30 m × 0.53 mm). High-purity helium (He, 99.999%) served as the carrier gas, with a barrier discharge ionization detector (BID) employed for detection. After 7 h of reaction, the catalyst dispersion was collected. The liquid products were filtered through a 0.2 μm membrane and quantified by high-performance liquid chromatography (HPLC, LC5090Plus, Fuli, China) using a ChromCore™ Sugar-10H column (6 μm, 7.8 × 300 mm). The mobile phase consisted of 5 mM H_2SO_4, with detection performed by a refractive index detector (RID-20A, Shimadzu, Japan).

The selectivity of C_2H_5OH ($^{S_{C_2H_5OH}}$) are calculated with below equations:

$$S_{C_2H_5OH} = \frac{12 \times \text{Yield}(C_2H_5OH)}{12 \times \text{Yield}(C_2H_5OH) + 8 \times \text{Yield}(CH_4) + 2 \times \text{Yield}(CO)}$$

1.5 DRIFTS measurements

DRIFTS measurements were conducted using a Thermo Scientific Nicolet FTIR spectrometer equipped with a liquid nitrogen cooled HgCdTe (MCT) detector. The spectra were obtained by applying an average of 128 scans with a spectral resolution of 2 cm^{-1}. The final spectra were obtained with the background spectra removed.

DRIFTS for CO Adsorption: the chamber was purged with N_2 (99.999%) at room temperature (RT) for 30 min to eliminate air after loading the samples and then background spectrum was recorded. Subsequently, pure CO (99.999%) was purged through until adsorption equilibrium was reached. Then CO was stopped by purge N_2 into the chamber to remove the CO in the gas phase.

DRIFTS for In Situ CO_2 Reaction: the reaction chamber was purged with N_2 (99.999%) at 100℃ for 30 min to remove moisture and air on the sample and then cooled to RT. After recording the background spectrum in N_2, CO_2 (99.999%) and H_2O vapor via bubbling of CO_2 gas through water were introduced into the reaction chamber until adsorption equilibrium was reached. Then the chamber was sealed and the spectra were recorded at certain time intervals under illumination of a 300 W Xe lamp with AM 1.5 filter.

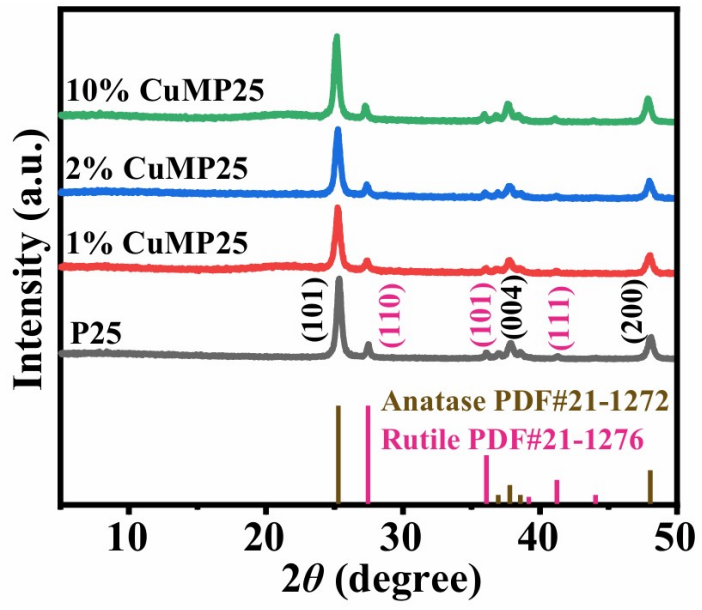

Fig. S1. XRD patterns of P25, 1% CuMP25, 2% CuMP25, and 10% CuMP25.

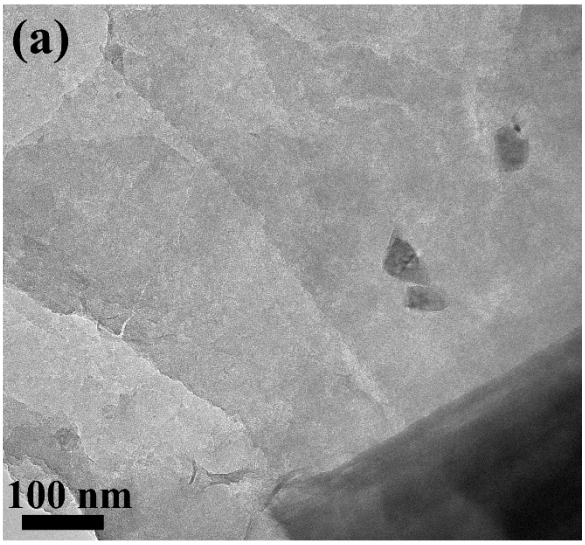

Fig. S2. TEM images of M after exfoliation.

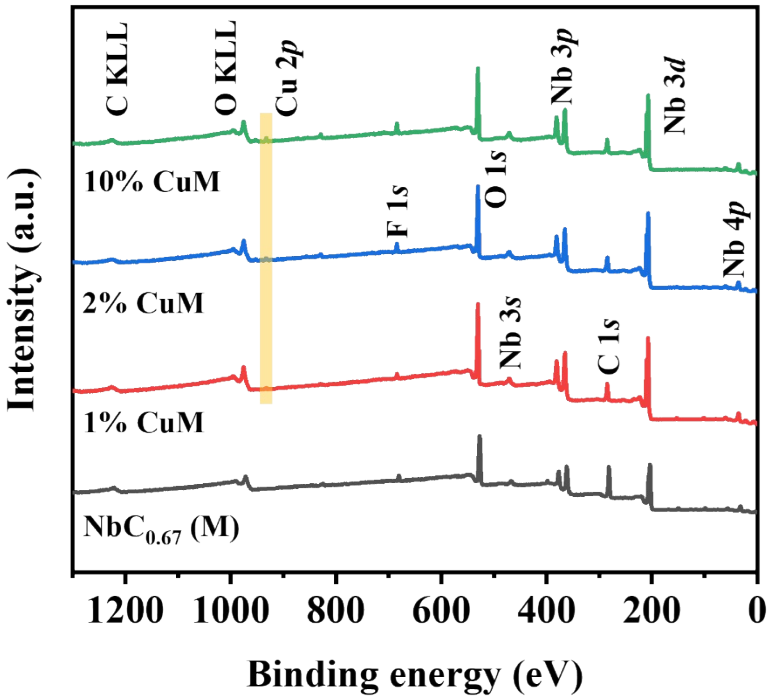

Fig. S3. XPS survey spectra corresponding to M and CuM.

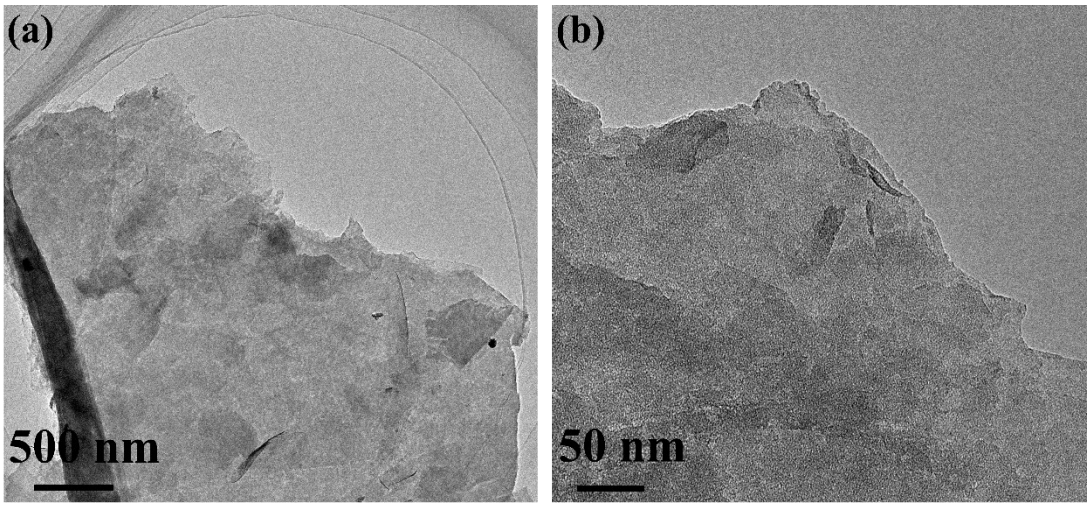

Fig. S4. TEM images of 2% CuM.

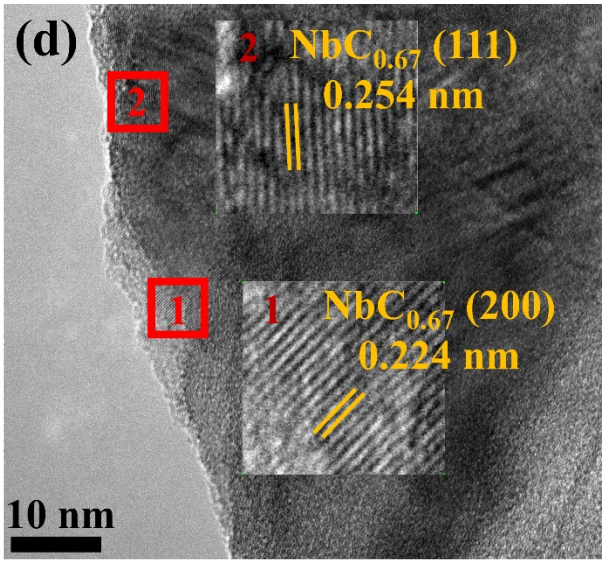

Fig. S5. HRTEM images of 2% CuM.

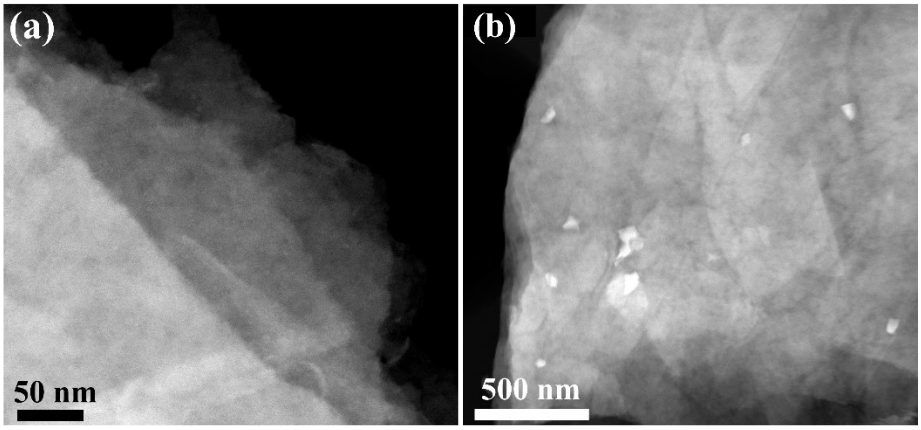

Fig. S6. HAADF-STEM image of 2% CuM.

Table S1. Atomic concentrations for M and CuM by XPS.

Atomic Concentration at. %					
Sample	Nb 3*d*	C 1*s*	Cu 2*p*	O 1*s*	F 1*s*
$NbC_{0.67}$	19.35	40.44	/	30.49	2.27
1% Cu-$NbC_{0.67}$	18.06	30.86	0.10	49.25	1.73
2% Cu-$NbC_{0.67}$	18.02	30.7	0.19	46.42	3.25
10% Cu-$NbC_{0.67}$	18.05	29.5	0.47	46.66	3.94

Table S2. Comparison on the activity and selectivity for photocatalytic CO_2 reduction in this work.

Photocatalysts	Yield in 0.1 M $NaHCO_3$ ($\mu mol\ g^{-1}\ h^{-1}$)		$S_{C_2H_5OH}$	Yield in H_2O ($\mu mol\ g^{-1}\ h^{-1}$)		$S_{C_2H_5OH}$
	C_2H_5OH	CH_4		C_2H_5OH	CH_4	
MP25	2.0	2.10	58.8%	0	3.50	0
1% CuMP25	9.6	0.23	98.4%	2.6	0.46	89.5%
2% CuMP25	25.9	0.74	98.1%	10.9	0.15	99%
10% CuMP25	13.5	0.14	99.3%	76.3	0.16	99.9%
20% CuMP25				4.9	0.10	55.0%

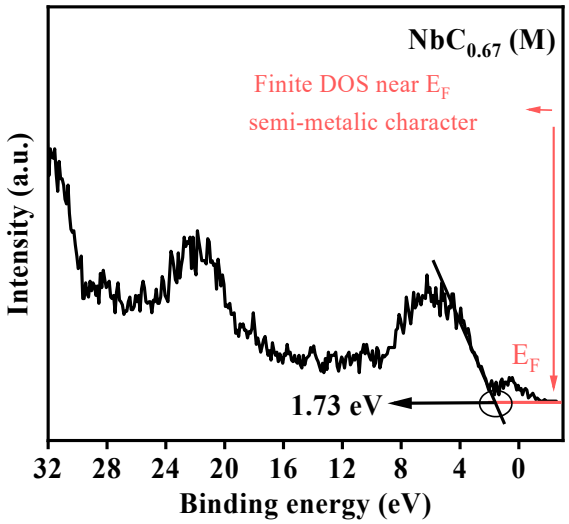

Fig. S7. XPS valence band spectrum of defective $NbC_{0.67}$ MXene (M).

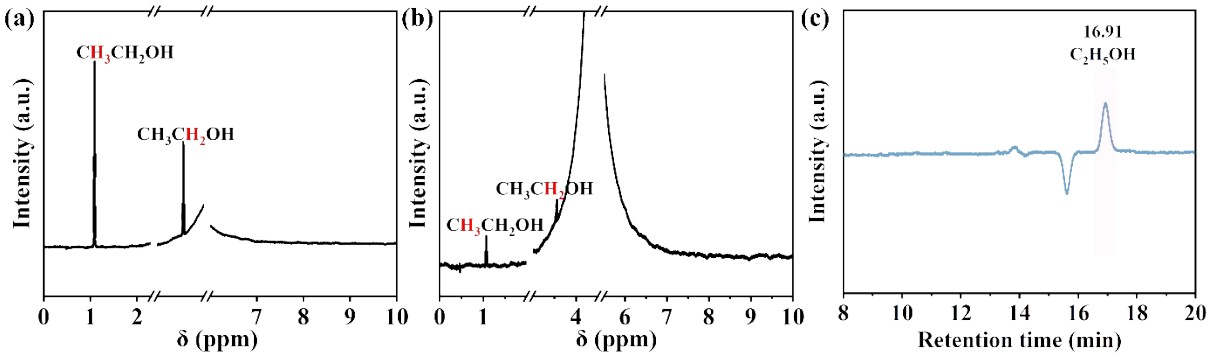

Fig. S8. (a) ^{1}H-NMR of ethanol standard sample; (b) ^{1}H-NMR of the reaction solution after photocatalytic reduction of 1% CuMP25 in H_2O for 7 hours.

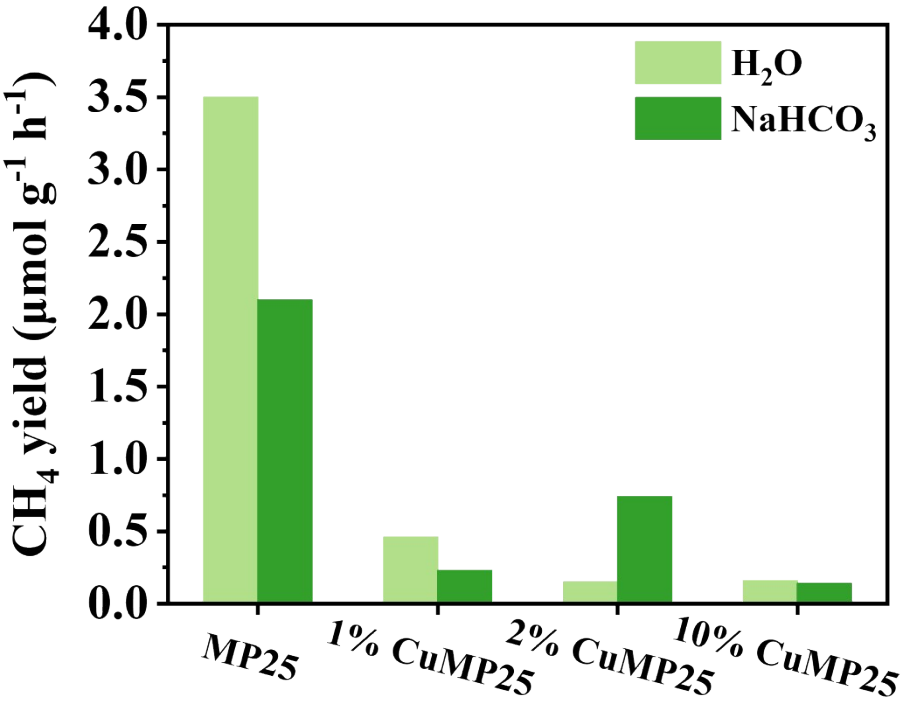

Fig. S9. The yields of methane for each sample after 7 hours of photocatalytic CO_2 reduction.

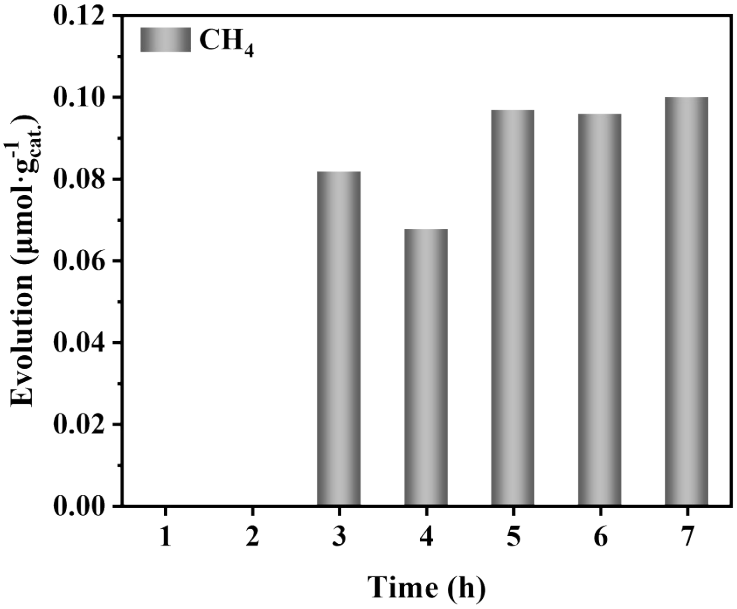

Fig. S10. Photocatalytic CO_2 conversion performance over reaction time using 20% CuMP25.

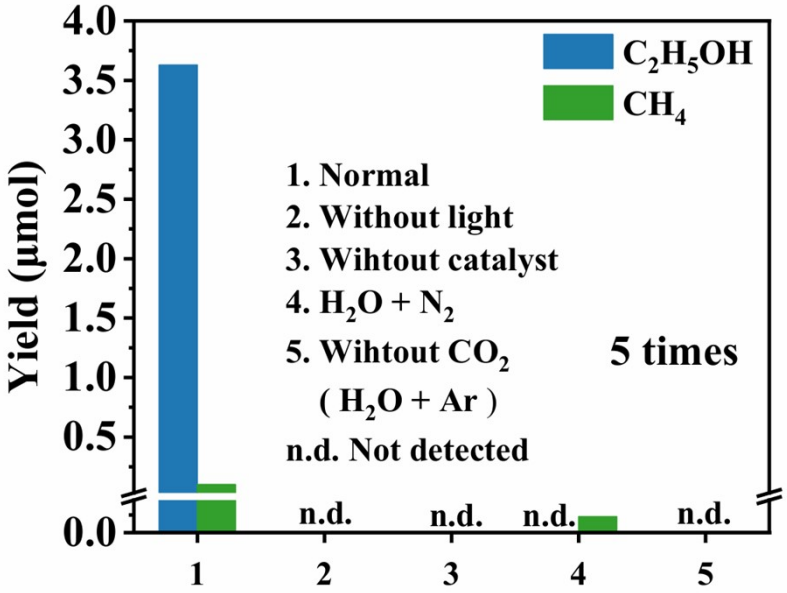

Fig. S11. Reference experiments for photocatalytic CO_2 reduction under different conditions: (1) normal CO_2 + H_2O + catalyst + light; (2) without light; (3) without catalyst; (4) H_2O + N_2; (5) H_2O + Ar (without CO_2). n.d. = not detected. The absence of ethanol and methane under Ar atmosphere confirms that the carbon source is exclusively derived from CO_2.

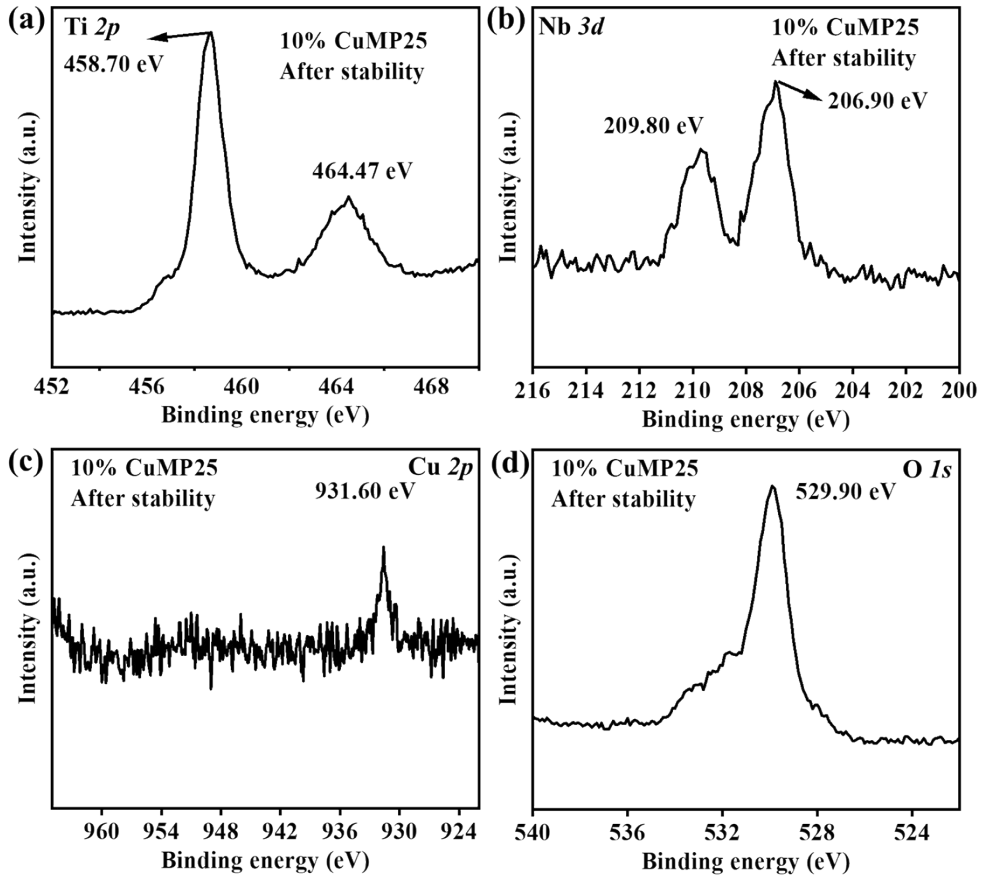

Fig. S12. Post-catalysis XPS analysis of 10% CuMP25 after three photocatalytic cycles: (a) Ti 2p, (b) Nb 3d, (c) Cu 2p, and (d) O 1s.

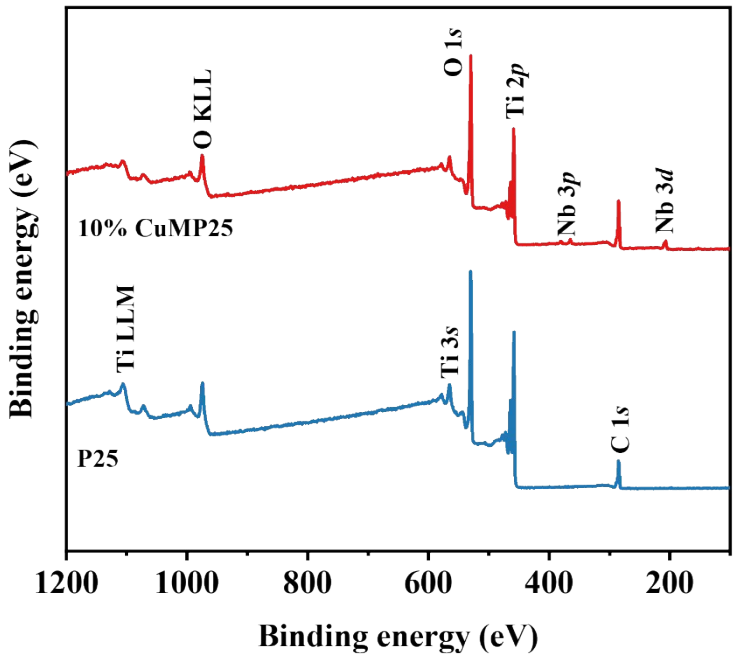

Fig. S13. XPS survey spectra corresponding to P25 and 10% CuMP25.

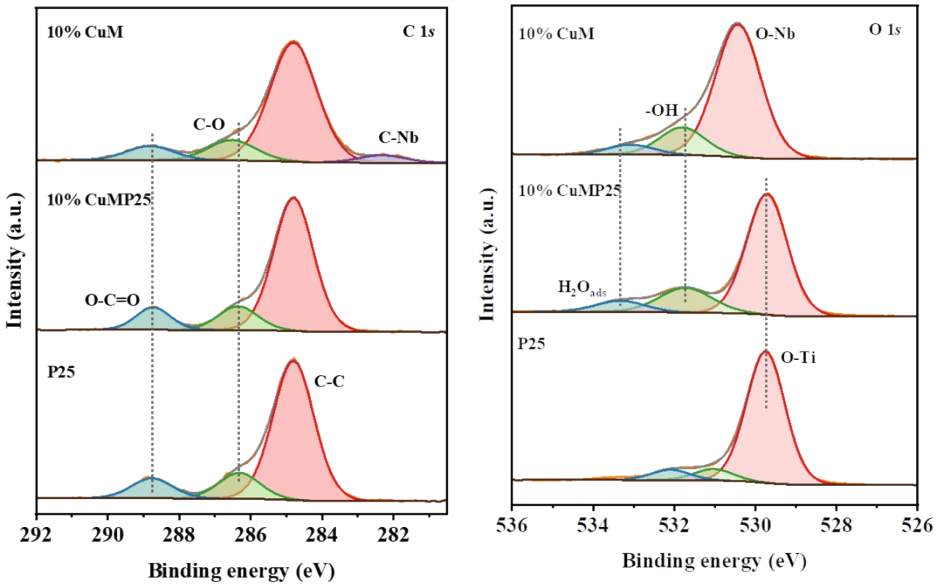

Fig. S14. High resolution XPS spectra of P25 and 10% CuMP25: (a) C 1*s*； (b) O 1*s*.

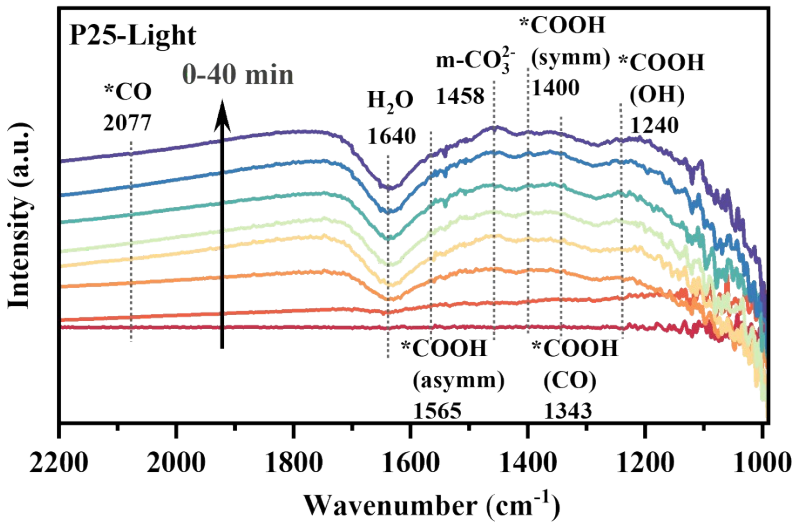

Fig. S15. *In situ* DRIFTS spectra taken during photocatalytic CO_2 reduction of P25.

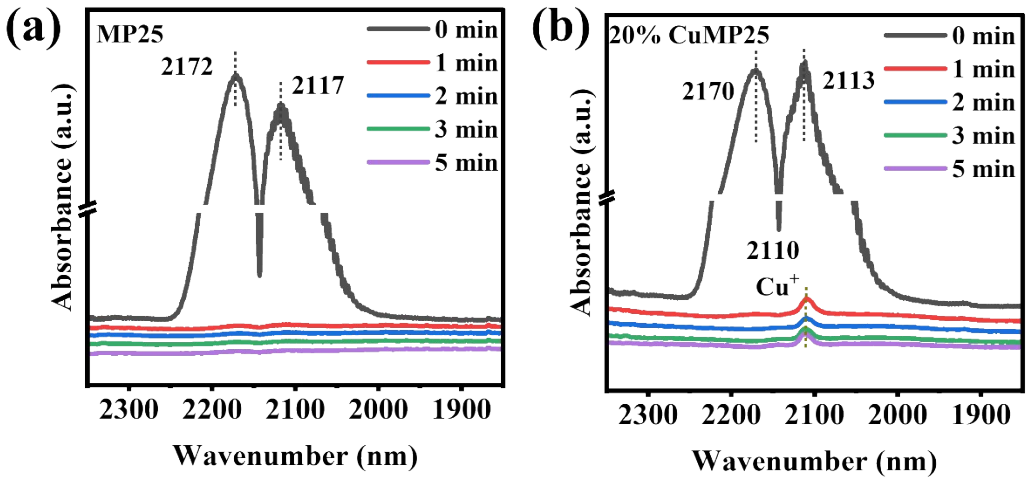

Fig. S16. CO-DRIFTS for (a) MP25 and (b) 20% CuMP25.

Table S3. Comparison of photocatalytic CO_2-to-ethanol performance.

Catalyst	Medium	Light	Ethanol rate ($\mu mol.g^{-1}.h^{-1}$)	Product selectivity (%)	Ref.
Ti_3C_2/CeO_2 (5-TC/Ce)	H_2O	Visible	~1225	98	[1]
C_3N_4 (Cu_4/Cu_1@CN)	H_2O	Visible	154	98	[2]
Cu SAs/UiO-66-NH_2	H_2O + TEOA	Visible	4.22	-	[3]
$CeO_2/CuO/TiO_2$	H_2O	UV–Vis	30.5	-	[4]
$Ag/Ag_2S/Ti_3C_2Tx$	H_2O	300 W Xe	125.3	-	[5]
$ZnCo_2O_4/ZnO$	H_2O	300 W Xe lamp	4.99	-	[6]
$In_2O_3/Cu–O_3$	H_2O	Visible	20.7	85.8	[7]
Cu_2O-Bi_2O_3-Bi	H_2O	300 W xenon lamp	145.66	91	[8]

ZnS/Co_3S_4	H_2O	AM 1.5G	20.62	-	[9]
10%CuMP25	H_2O	AM 1.5	76.3	99.9	This wrok

References

[1] R. P. Mishra, M. Mrinalini, N. Kumar, S. Bastia, Y. S. Chaudhary, *Langmuir* **2023**, *39*, 14189.

[2] Z. Guo, H. Yang, X. Huang, Y. Ning, H. Luo, J. Xie, J. He, Y. Liu, T.-C. Lau, *Angew. Chemie Int. Ed.* **2025**, *64*, e202423666.

[3] G. Wang, C.-T. He, R. Huang, J. Mao, D. Wang, Y. Li, *J. Am. Chem. Soc.* **2020**, *142*, 19339.

[4] P. Seeharaj, N. Vittayakorn, J. Morris, P. Kim-Lohsoontorn, *Nanotechnology* **2021**, *32*, 375707.

[5] B. Zhang, Y. Chen, F. Li, Y. Zhang, X. Li, W. Xiong, W. Dai, *Nanoscale Adv.* **2025**, *7*, 1195.

[6] H. Ma, X. Wu, X. Li, J. Liu, H. Dong, Y. Liu, L. Niu, F. Zhang, W. Wang, C. Shao, X. Li, Y. Liu, *Inorg. Chem.* **2024**, *63*, 15735.

[7] S. Gong, B. Ni, X. He, J. Wang, K. Jiang, D. Wu, Y. Min, H. Li, Z. Chen, *Energy Environ. Sci.* **2023**, *16*, 5956.

[8] Y. Zhou, P. Cao, H. Bai, M. I. Ahmad, S. Chen, Y. Liu, H. Yu, X. Quan, *Appl. Catal. B Environ. Energy* **2026**, *380*, 125780.

[9] X. Shi, Y. Sun, K. Lai, L. Li, N. Li, Y. Gao, L. Ge, *Appl. Catal. B Environ. Energy* **2026**, *382*, 126001.